AGU PUBLICATIONS

JGR

Journal of Geophysical Research: Space Physics

RESEARCH ARTICLE
10.1002/2015JA021539

Key Points:
- Importance of interstellar hydrogen ionization in the heliosheath
- Estimates of photoionization and electron impact ionization in the heliosheath
- Effect of ionization on plasma flows in the heliosheath and ENA imaging

Correspondence to:
M. Gruntman,
mikeg@usc.edu

Citation:
Gruntman, M. (2015), Interstellar hydrogen ionization in the heliosheath, *J. Geophys. Res. Space Physics*, *120*, 6119–6132, doi:10.1002/2015JA021539.

Received 5 JUN 2015
Accepted 24 JUL 2015
Accepted article online 28 JUL 2015
Published online 25 AUG 2015

Interstellar hydrogen ionization in the heliosheath

Mike Gruntman[1]

[1]Department of Astronautical Engineering, University of Southern California, Los Angeles, California, USA

Abstract The expanding solar wind plasma undergoes a shock transition at the interstellar boundary of the solar system and fills the inner heliosheath, the region between the termination shock and the heliopause. The nonequilibrium heliosheath plasma is a main source of energetic neutral atoms that allow remote probing of the heliospheric interface region. Global models of the heliosphere interaction with the interstellar medium often disregard solar photoionization and electron impact ionization of interstellar gas in the heliosheath. When ionization is included, it is commonly treated in a simplified manner and complexity of heliospheric interactions obscures its effect on the properties of the plasma. This work concentrates on physical estimates of ionization and shows that it may lead to significant mass loading of plasma flows in the heliosheath. In turn, mass loading would slow down plasma flows and deplete populations of nonthermal energetic protons. The magnitude of the effect depends on poorly understood and largely unknown energy transfer to electrons at the termination shock and beyond. The presented estimates show that inclusion of ionization is indispensable for global heliospheric modeling and for interpretation of heliosphere imaging in fluxes of energetic neutral atoms.

1. Introduction

Complex interaction of the solar wind with the local interstellar medium (LISM) creates the heliosphere. The relative motion of the LISM with respect to the Sun, often described as the interstellar wind, results in a pronounced nose-tail asymmetry of the heliosphere. Interstellar magnetic field also adds important asymmetry to the interaction region.

The supersonic solar wind plasma undergoes a shock transition at large heliocentric distances and fills the region between the termination shock and the heliopause, the inner heliosheath. (Throughout the article, the word heliosheath is used in the sense of the "inner heliosheath.") There, the plasma flows into the heliospheric tail where it eventually mixes with the surrounding LISM. Protons of the shocked plasma charge exchange on background interstellar hydrogen atoms in the heliosheath, producing energetic neutral atoms (ENAs). Measurement of these energetic atoms is the basis for heliosphere imaging in ENA fluxes which opens a way to remotely probe the interstellar boundary of the solar system [*Patterson et al.*, 1963; *Gruntman and Leonas*, 1983; *Gruntman et al.*, 1990; *Hsieh et al.*, 1991; *Gruntman*, 1992; *Roelof*, 1992; *Hsieh and Gruntman*, 1993; *Gruntman*, 1997; *Gruntman et al.*, 2001; *Fahr et al.*, 2007; *McComas et al.*, 2009b].

Voyager 1 and 2 spacecraft crossed the termination shock at 94 AU and 84 AU in 2004 and 2007, respectively, and entered the heliosheath [e.g., *Decker et al.*, 2005; *Stone et al.*, 2005; *Decker et al.*, 2008; *Richardson et al.*, 2008; *Stone et al.*, 2008]. Then in 2012, Voyager 1 observations suggested that it had reached the heliopause at the distance of 122–123 AU from the Sun [e.g., *Burlaga et al.*, 2013; *Krimigis et al.*, 2013; *Stone et al.*, 2013]. Launched in 2008, the Interstellar Boundary Explorer (IBEX) mission obtained first maps of the heliospheric interface in ENA fluxes [*McComas et al.*, 2009b] which revealed details of the global solar wind interaction with the surrounding LISM. Cassini spacecraft also imaged the heliosphere in ENA fluxes at somewhat higher energies of atoms [*Krimigis et al.*, 2009].

In situ measurements by Voyagers and remote observations by IBEX and Cassini found a number of unexpected phenomena at the interstellar boundary of the solar system. The concept of heliosphere ENA imaging [*Gruntman et al.*, 2001], including its implementation in a space experiment for remote probing of the heliosheath and predicted intensities of atom fluxes, were all soundly validated by the IBEX mission [*McComas et al.*, 2009a, 2009b] that also discovered a surprising standing-out band of enhanced ENA emissions across the sky, called the *ribbon* [*Funsten et al.*, 2009b; *McComas et al.*, 2009b; *Schwadron et al.*, 2009]. The existing understanding of heliospheric interactions at that time completely missed the latter phenomenon, and the ribbon had not been anticipated in the IBEX proposal [*McComas et al.*, 2009a] and

in the earlier dedicated mission proposals. (Heliosphere ENA imaging was first included as a main part of the larger "Interstellar Pathfinder" mission, Principal Investigator G. Gloeckler, proposed as Medium Explorer in 1998 and 2001 [*Moebius et al.*, 1998; *McComas et al.*, 2003].) While a number of hypotheses were suggested since the ribbon discovery [*McComas et al.*, 2009b, 2010], its definitive explanation has not been developed yet. At the same time, global heliospheric models achieved a high degree of sophistication (e.g., reviews by *Zank* [1999] and *Izmodenov and Baranov* [2006], and references therein). Failure of predicting and difficulties in reproducing the ribbon in simulations of heliospheric interactions suggest that some important physical phenomena may not be fully understood yet and/or they are included into models in oversimplistic ways.

Global flows of mass, momentum, and energy of the solar wind vary with time. It takes several years for the solar wind plasma to flow through the interface region and reach the distant heliospheric tail which should, to some degree, smooth out changes of heliosheath properties during solar cycles. Nevertheless, IBEX also revealed decrease of intensities of ENA fluxes, sometimes described as heliosphere "dimming" [*McComas et al.*, 2012, 2014]. Some correlations with the changing global solar wind properties have been noted, but their exact mechanisms remain unclear.

Understanding properties of the shocked solar wind plasma between the termination shock and heliopause is indispensable for explaining heliospheric ENA images in the 0.5–6.0 keV energy range obtained by the IBEX-Hi instrument [*Funsten et al.*, 2009a, 2009b] on IBEX. Even most sophisticated global models introduce important simplifications. Most common assumptions include multifluid and magnetohydrodynamic descriptions of flows of gases and plasmas, and Maxwellian or other postulated velocity distributions of plasma protons immediately downstream of the termination shock [e.g., *Zank*, 1999; *Fahr et al.*, 2000; *Izmodenov*, 2000; *Izmodenov and Baranov*, 2006; *Malama et al.*, 2006; *Opher et al.*, 2006; *Fahr et al.*, 2007; *Pogorelov et al.*, 2008; *Izmodenov et al.*, 2009; *Zank et al.*, 2009; *Alouani-Bibi et al.*, 2011; *Ratkiewicz et al.*, 2012; *Heerikhuisen et al.,* 2014; *Opher et al.*, 2015; and references therein]. Physical simplifications and assumptions lead to uncertainties in comparing results of model simulations with observations which are hard to quantify and they are rarely, if ever, pointed out and discussed in publications.

Voyager in situ measurements of the bulk solar wind plasma and higher-energy ($>$20 keV) protons [e.g., *Decker et al.*, 2005, 2008; *Richardson et al.*, 2008] incompletely characterize the termination shock that may also differ from conventional shock structures [e.g., *Zank*, 1999; *Izmodenov and Baranov*, 2006; *Fahr et al.*, 2007; *Roelof et al.*, 2010; *Chalov and Fahr*, 2013]. Beyond the shock, the heliosheath plasma is not in equilibrium, with nonthermal, often called suprathermal, protons ($E > 0.5$ keV) accounting for most energy density while most mass being in relatively cold protons [*Funsten et al.*, 2009b; *Krimigis et al.*, 2009; *Roelof et al.*, 2010; *Schwadron et al.*, 2011; *Richardson and Decker*, 2015]. The plasma may not even be stationary due to variations of the global solar wind properties. Coulomb collisions are so rare in the heliosheath, even among electrons, that they could be disregarded.

The complexity of global interactions of the solar wind with the LISM obscures and makes it difficult to assess relative importance of particular physical processes. For example, many otherwise sophisticated and complex models of the heliospheric interactions disregard solar photoionization and electron impact ionization in the heliosheath [e.g., *Zank*, 1999 and references therein; *Zank et al.*, 2009; *Alouani-Bibi et al.*, 2011; *Ratkiewicz et al.*, 2012; *Heerikhuisen et al.,* 2014]. Photoionization is often considered negligible, while electron impact ionization either tacitly assumed inconsequential or too complex and uncertain for inclusion into models.

This work specifically concentrates on physical estimates of ionization of interstellar hydrogen at large distances from the Sun beyond the termination shock. The estimates show that both photoionization and electron impact ionization could significantly affect properties of the heliosheath plasma. The magnitude of the latter process depends on electron properties which are poorly constrained by observations and remain largely unknown. So we first consider mass loading of plasma flows caused by photoionization in the heliosheath and then use it as a yardstick to assess possible effects of electron impact ionization. The estimates suggest that inclusion of ionization into global modeling is indispensable for understanding details of the heliospheric interaction and particularly for interpretation of heliospheric ENA images.

2. Photoionization in the Heliosheath

The solar wind and solar electromagnetic radiation could disturb properties of gas and plasma at large distances from the Sun beyond the termination shock. The effect of solar photoionization on the interstellar

wind is relatively small and can be usually disregarded. It is recognized as important, however, for properties of interstellar neutral atoms closer to the Sun inside the heliosphere [e.g., *Zank et al.*, 2009; *Bochsler et al.*, 2014; *Izmodenov et al.*, 2013].

The Solar Irradiation Platform (SIP) provides solar spectra on a daily basis and allows one to calculate typical photoionization rates and photoelectron energies for different levels of solar activity. (SIP historical irradiances are provided courtesy of W. Kent Tobiska and Space Environment Technologies; http://www.spacewx.com.) For typical low solar activity, as on 1 January 2008, with the solar $F_{10.7}$ index being 79 on that day, the photoionization rate of atomic hydrogen at 1 AU was $8.13 \times 10^{-8}\,s^{-1}$ with the average photoelectron energy 4.14 eV for the solar spectrum provided by SIP. For conditions of very high solar activity, as observed on 1 January 2002, with the $F_{10.7}$ index equal 232, the photoionization rate was $1.42 \times 10^{-7}\,s^{-1}$ and the average photoelectron energy was 5.0 eV. During moderate solar conditions, the photoionization rate at 1 AU is close to $1.0 \times 10^{-7}\,s^{-1}$ and photoelectron energy is about 4.2 eV. Absorption and attenuation of the solar extreme ultraviolet radiation on the heliospheric scales are negligible. So the hydrogen atom photoionization rate β_S depends on the heliocentric distance R as

$$\beta_S(R) = \beta_{S,0}\left(\frac{R_0}{R}\right)^2,$$

where $\beta_{S,0}$ is the photoionization rate at $R_0 = 1$ AU. The subscript S here and below refers to solar photoionization; the subscript e would refer to processes due to electron impact ionization.

Consider, for example, interstellar hydrogen atoms approaching the solar system with the interstellar wind velocity 25 km s^{-1}. (In this work, we assume that the partially ionized LISM consists of neutral atomic hydrogen, protons, and electrons only.) A small fraction, about 0.5%, of interstellar atoms would be ionized when they reach the heliocentric distance 130 AU under moderate solar conditions. For a LISM with neutral atoms twice more abundant than protons, photoionization would increase interstellar plasma temperature (by adding energetic photoelectrons) by about 100 K and slow it down (by mass loading) by 100 m s^{-1} at this distance. These effects on the LISM flow are small and could be disregarded in most considerations.

Note that energetic neutral atoms in the solar wind cause a most important disturbance of the interstellar wind [*Gruntman*, 1982]. Even if the interstellar plasma flow is supersonic and thus "unaware" of a heliosphere obstacle in front of it, ENAs significantly modify the LISM properties upstream of a bow shock. In fact, the usually referred to "pristine" interstellar medium surrounding the Sun is "contaminated" and disturbed by our star to large heliocentric distances.

Charge exchange of ions of the supersonic solar wind on interplanetary neutral gas creates a neutral component in the solar wind, sometimes called the neutral solar wind [*Fahr*, 1968; *Banks*, 1971; *Holzer*, 1977; *Gruntman*, 1980; *Gruntman*, 1982; *Gruntman and Leonas*, 1983, 1986; *Gruntman et al.*, 1990; *Bleszynski et al.*, 1992; *Gruntman*, 1994, 1997; *Fahr et al.*, 2007]. The neutral solar wind atoms penetrate into the surrounding LISM for several hundred astronomical units and heat and slow down the approaching interstellar plasma [*Gruntman*, 1982]. Global heliospheric modeling began to include this effect from 1990s [*Baranov and Malama*, 1993] and later also added ENAs emitted by the heliosheath plasma and acting on the LISM in a similar way. One suggested explanation of the ribbon [*Chalov et al.*, 2010; *Heerikhuisen et al.*, 2010] derives from possible consequences of the neutral solar wind effect on the LISM.

Solar photoionization is not particularly important for modifying properties of interstellar neutral populations inside the heliosheath. It could, however, produce a significant effect on the rarified heliosheath plasma because it is 2 orders of magnitude less denser than the neutral interstellar gas of the LISM. Photoionization of interstellar hydrogen atoms passing through the heliosheath creates protons and electrons. The heliosheath plasma flow picks up these new charged particles, resulting in mass loading of the flow. Electron impact ionization of atoms also leads to mass loading. While one can include photoionization into modeling in a straightforward way, accounting for electron impact ionization, as we will see below, presents difficulties.

Consider a typical simplified axisymmetric heliospheric interaction shown in Figure 1, with a bow shock, heliopause, and termination shock. The polar angle θ is counted from the upwind (interstellar wind) direction, and heliocentric distances to the termination shock and heliopause are $R_{TS}(\theta)$ and $R_{HP}(\theta)$, respectively. The heliosheath plasma (gray region in Figure 1) flows across (not necessarily normally) a side surface of a cone

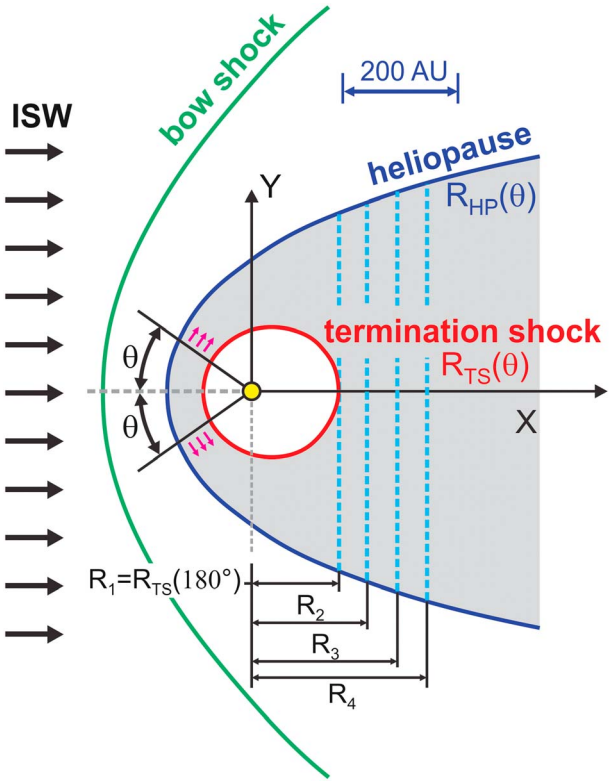

Figure 1. Schematic of typical simplified axisymmetric heliospheric interaction with the bow shock (green line), heliopause (dark blue), and termination shock (red); the positions and shapes of the surfaces were calculated by *Izmodenov et al.* [2003]. The angle θ is counted from the upwind (interstellar wind) direction. We consider the heliosheath plasma (gray) flow across the surface of a cone with a half-angle θ in the upwind hemisphere and across plane sections at heliocentric distances $R_1 = 150$ AU, $R_2 = 200$ AU, $R_3 = 250$ AU, and $R_4 = 300$ AU in the tail.

with the half-angle θ between heliocentric distances $R_{TS}(\theta)$ and $R_{HP}(\theta)$. All the solar wind flow that crosses the termination shock at angles $< \theta$ would be evacuated to the heliospheric tail through this side surface of the cone.

The Goddard Space Flight Center/Space Physics Data Facility OMNI database (http://omniweb.gsfc.nasa.gov) provides solar wind properties at 1 AU in the ecliptic plane. *McComas et al.* [2008] argued that variations of the averaged solar wind total mass, momentum, and energy fluxes at the ecliptic were approximately representative for all heliolatitudes. So in this work, we assume the isotropic solar wind consisting of only protons and electrons with the number density n_{SW} at $R_0 = 1$ AU and velocity V_{SW} independent of the heliocentric distance. The corresponding solar wind flux number density is $f_0 = n_{SW}V_{SW}$ at 1 AU, and it is inversely proportional to the square of the heliocentric distance.

The total solar wind mass outflow (the number of protons per second) $\Phi(\theta)$ into a cone with the half-angle θ (Figure 1) would then be

$$\Phi(\theta) = 2\pi(1 - \cos\theta)R_0^2 f_0.$$

The rate of production, $\alpha_S(\theta)$, of proton-electron pairs by photoionization in the heliosheath region restricted by the same half-angle θ is

$$\alpha_S(\theta) = \int_0^{\theta}\int_{R_{TS}(\theta)}^{R_{HP}(\theta)} n_0(R,\theta)\beta_S(R)2\pi R^2 \sin\theta \mathrm{d}R\mathrm{d}\theta,$$

where $n_0(R,\theta)$ is the number density of interstellar hydrogen atoms. Assuming, for simplicity, the uniform number density, $n_0(R,\theta) = n_0 = \text{const}$, one obtains

$$\alpha_S(\theta) = 2\pi n_0 \beta_{S,0} R_0^3 \Gamma(\theta),$$

where the dimensionless parameter,

$$\Gamma(\theta) = \frac{1}{R_0}\int_0^{\theta}[R_{HP}(\theta) - R_{TS}(\theta)]\sin\theta \mathrm{d}\theta,$$

characterizes the geometric properties of the heliosheath.

Let us define the mass loading coefficient (ratio) of the plasma flow, $\gamma_S(\theta)$, as the ratio of the additional photoionization-produced plasma mass flow to that of the solar wind across a side cone surface of the heliosheath region restricted by the half-angle θ. Then,

$$\gamma_S(\theta) = \frac{\alpha_S(\theta)}{\Phi(\theta)} = g_0 \frac{\Gamma(\theta)}{1 - \cos\theta},$$

where the dimensionless coefficient

$$g_0 = \frac{n_0 \beta_{S,0} R_0}{f_0}$$

describes solar and interstellar conditions and is independent of the heliosheath geometric properties.

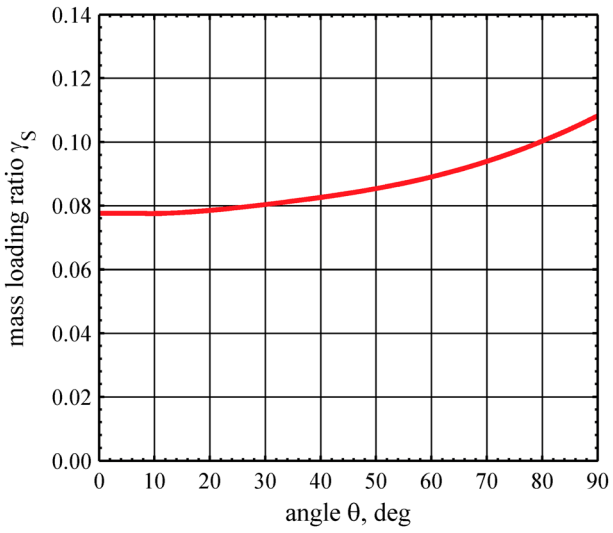

Figure 2. Angular dependence of the mass loading coefficient $\gamma_S(\theta)$ due to photoionization.

Let us consider, as an example, a representative heliospheric interface geometry shown in Figure 1 as calculated by *Izmodenov et al.* [2003] for realistic parameters of the LISM and the solar wind. For the upwind direction, the distances to the termination shock, heliopause, and bow shock are 89 AU, 152 AU, and 270 AU, respectively. In general, exact parameters of the interstellar medium and the solar wind used in simulations are not particularly important for the purposes of this work as we focus on nonstrictly self-consistent physical estimates of ionization effects for a typical geometry.

Let us assume the hydrogen atom photoionization rate $\beta_{S,0} = 1.0 \times 10^{-7}$ s^{-1} and the solar wind flux density $f_0 = 2.2 \times 10^8$ cm^{-2}s^{-1} at 1 AU. Such parameters were average for solar conditions from 2007 to 2013, the time interval important for IBEX ENA measurements. The corresponding photoionization rates at the heliocentric distances of 100 AU (characteristic distance to the termination shock) and 150 AU (characteristic distance to the heliopause) would be $\beta_{S,100} = 1.0 \times 10^{-11}$ s^{-1} and $\beta_{S,150} = 0.44 \times 10^{-11}$ s^{-1}, respectively. Let us also adopt the typical number density of neutral interstellar hydrogen $n_0 = 0.18$ cm^{-3} as in simulations of *Izmodenov et al.* [2003] for some consistency with the used heliosphere geometry. For these selected solar and interstellar conditions, one obtains the coefficient $g_0 = 0.00122$.

Figure 2 shows the angular dependence of the mass loading coefficient that increases from $\gamma_S = 0.078$ at small angles to $\gamma_S = 0.108$ at $\theta = 90°$. So photoionization would increase the heliosheath plasma mass flow by approximately one tenth when it reaches and crosses the annulus at $\theta = 90°$.

Consider also plane sections cutting through the solar wind flow at certain heliocentric distances in the heliotail (Figure 1). The entire solar wind mass output flows through these sections, and photoionization of interstellar hydrogen in the corresponding regions of the heliosheath contributes to mass loading. As an example, the mass loading coefficients would be $\gamma_{S,1} = 0.129$, $\gamma_{S,2} = 0.151$. $\gamma_{S3,3} = 0.170$, and $\gamma_{S,4} = 0.182$ for sections (shown to scale in Figure 1) at heliocentric distances $R_1 = 150$ AU, $R_2 = 200$ AU, $R_3 = 250$ AU, and $R_4 = 300$ AU, respectively. So the mass flow of the solar wind increases, due to photoionization, by roughly one fifth in the heliotail by the distance of 300 AU from the Sun.

3. Electron Impact Ionization in the Heliosheath

First attempts to account for electron impact ionization of interstellar hydrogen atoms beyond the termination shock in global heliospheric models date back at least to work of *Baranov and Malama* [1996]. The process remains often disregarded in the heliosheath to this date which is sometimes justified by complexity of its inclusion into models [e.g., *Alouani-Bibi et al.*, 2011]. When this ionization is accounted for, global models usually assume Maxwellian distributions of electrons at plasma temperatures [*Izmodenov et al.*, 2003; *Izmodenov and Baranov*, 2006; *Malama et al.*, 2006; *Scherer et al.*, 2014].

The energy-dependent cross-section $\sigma_e(E_e)$ of electron impact ionization of hydrogen atoms [*Janev et al.*, 2003] peaks at $\sigma_e > 5.0 \times 10^{-17}$ cm^2 in the $E_e = 30 - 130$ eV energy range (Figure 3, top). For electrons with a Maxwellian velocity distribution at temperature T_e and negligible velocities of hydrogen atoms, the temperature-dependent ionization rate coefficient $c_e(T_e) = \langle \sigma_e V_e \rangle$ is obtained by averaging over electron thermal velocities V_e [*Janev et al.*, 1987].

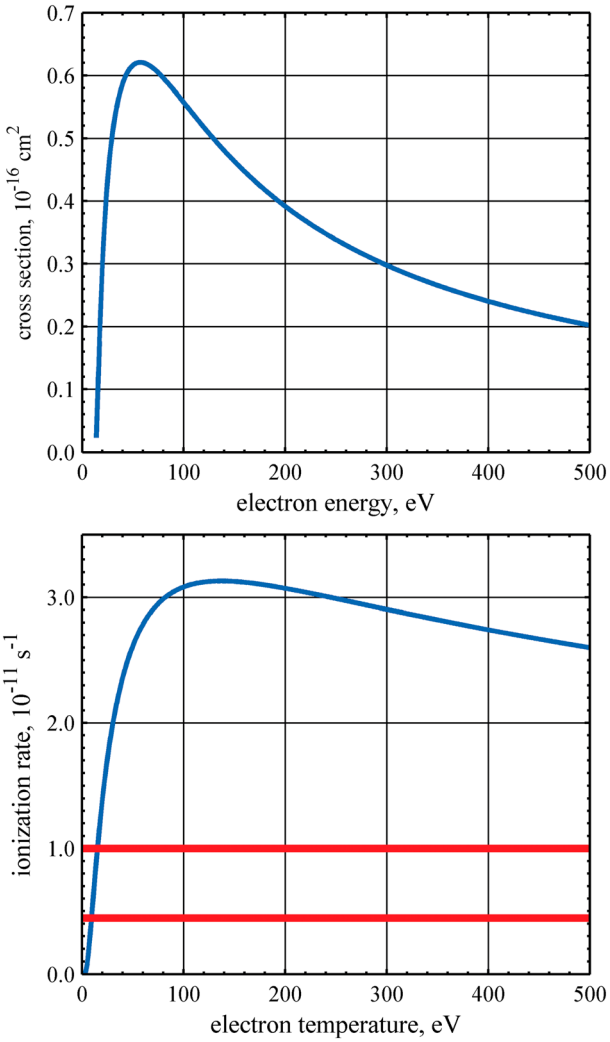

Figure 3. (top) Energy dependence of the hydrogen atom electron impact ionization cross-section $\sigma_e(E_e)$ and (bottom) temperature dependence of the ionization rate $\beta_e(T_e) = n_e\langle\sigma_e V_e\rangle$ of hydrogen atoms by electrons with a Maxwellian distribution of velocities and number density $n_e = 10^{-3}$ cm^{-3}. Two solid horizontal straight lines at the ionization rates $\beta_{S,100} = 1.0 \times 10^{-11}$ s^{-1} and $\beta_{S,150} = 0.44 \times 10^{-11}$ s^{-1} correspond to moderate solar activity photoionization rates of hydrogen atoms at 100 AU and 150 AU from the Sun, respectively.

Let us assume the uniform electron (and proton) number density in the heliosheath, $n_e = 10^{-3}$ cm^{-3}. It corresponds to the constant velocity solar wind with the number density $n_{SW} = 5$ cm^{-3} at 1 AU that doubles its number density in a termination shock transition at the heliocentric distance 100 AU. Voyager 2 spacecraft measured heliosheath plasma number densities varying (with the exception of several relatively short time intervals) in the 0.0008–0.0022 cm^{-3} range at heliocentric distances from 84 to 105 AU [*Richardson and Decker*, 2014, 2015].

Figure 3 (bottom) shows the temperature-dependent electron impact ionization rate of hydrogen atoms $\beta_e(T_e) = n_e c_e$. The rate rises rapidly with increasing temperatures at $T_e < 60$ eV, peaks at temperatures 134–138 eV, and then slowly decreases as temperatures increase up to several hundred eV. Figure 3 (bottom) also shows the moderate solar activity photoionization rates, $\beta_{S,100}$ and $\beta_{S,150}$, of atomic hydrogen at distances 100 AU and 150 AU from the Sun, respectively.

The only existing in situ plasma measurements in the heliosheath did not directly probe properties of electrons. One Faraday cup (side sensor D) of the Voyager 2 plasma instrument is sensitive to electrons with 10–5950 eV energies [*Bridge et al.*, 1977; *Scudder et al.*, 1981; *Sittler*, 1983]. Electron fluxes are too low, however, for reliable measurements in the distant solar wind and in the heliosheath (Richardson, private communications, 2015). It is also unclear how exactly absence of measurable electron fluxes constrains possible electron effective temperatures that could in principle range, as discussed below on the basis of the energy balance, from a few eV up to a few hundred eV. Therefore, it is not excluded that electron impact ionization could be larger than photoionization everywhere in the heliosheath, with an important effect on the plasma flow, if electron temperatures exceed 20–30 eV.

Ionization of interstellar hydrogen increases the number density of the heliosheath plasma. It also changes effective electron temperatures in the region and consequently electron impact ionization rates that depend on temperature. The average energy of photoelectrons produced by photoionization under moderate solar activity conditions is $\varepsilon_S = 4.2$ eV. Injection of such electrons into the heliosheath plasma would heat or cool its electron component depending on whether the temperature is lower than a few eV or higher than several eV, respectively. In addition, each act of electron impact ionization "removes" the hydrogen atom ionization energy, $\varepsilon_e = -13.6$ eV, from thermal motion of the electron population.

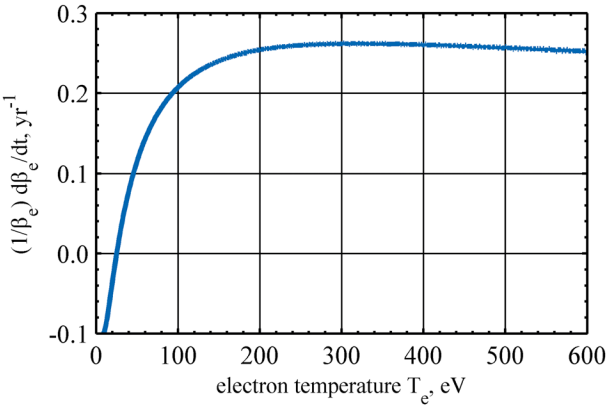

Figure 4. Relative electron impact rate change $(1/\beta_e)\, d\beta_e/dt$ as function of electron temperature T_e under typical solar and interstellar conditions assumed in this article.

The concept of heating or cooling of the bulk plasma electrons is applicable only if photoelectrons reach a local equilibrium with a Maxwellian velocity distribution. Such Maxwellization is not necessarily what happens in the plasma of the heliosheath where Coulomb collisions are rare and negligible. So it is not excluded that new electrons preserve their energies to some extent. Then photoionization, for example, could create a separate population of electrons with energies 0–50 eV in the heliosheath plasma, with abundances ~10% at $\theta = 90°$ and ~20% in the heliotail.

Let us assume instantaneous accommodation and Maxwellization of new electrons by the plasma electron component; also, let us assume the initial electron temperature T_e at least several eV. Ionization of interstellar hydrogen then results in increase of the number density of electrons and decrease of their temperature. The electron impact ionization rate increases proportionally to the electron number density. The decrease in electron temperature either increases or decreases the ionization rate depending on whether the initial electron temperature is higher than ~140 eV or lower than ~130 eV, respectively.

The total ionization rate, α, of interstellar hydrogen, the sum of photoionization and electron impact ionization, is

$$\alpha = \beta_S + \beta_e = \beta_S(1 + \xi),$$

where $\xi = \beta_e/\beta_S = c_e n_e/\beta_S$ is the ratio of local electron impact ionization and photoionization rates. The photoionization rate, β_S, is independent of plasma conditions and time. In contrast, the electron impact ionization rate, β_e, depends on the time-varying local electron number density and temperature. Noting that the rate of change of the electron number density is

$$\frac{dn_e}{dt} = n_0\beta_S(1 + \xi)$$

and expressing the rate of temperature change through the properties of photoelectrons and energy losses in electron impact ionization, one then readily obtains the relative rate of change of β_e,

$$\frac{1}{\beta_e}\frac{d\beta_e}{dt} = n_0\left[\frac{\tau_S + \xi\tau_e - (1+\xi)\,T_e}{\xi}\,\frac{dc_e}{dT_e} + c_e\,\frac{1+\xi}{\xi}\right],$$

where $\tau_S = 2\varepsilon_S/(3k_B)$ and $\tau_e = 2\varepsilon_e/(3k_B)$ are temperatures associated with new electrons for processes of photoionization and electron impact ionization, respectively, and k_B is the Boltzmann constant; note that $\tau_S > 0$ and $\tau_e < 0$. When electron impact ionization dominates, $\beta_e \gg \beta_S$ or $\xi \gg 1$, then

$$\frac{1}{\beta_e}\frac{d\beta_e}{dt} \approx n_0\left[(\tau_e - T_e)\frac{dc_e}{dT_e} + c_e\right].$$

Figure 4 shows the temperature dependence of the relative rate change $(1/\beta_e)\, d\beta_e/dt$ for the adopted in this work interstellar and solar parameters, n_0, n_e, and $\beta_S = \beta_{S,100}$. It is negative, and the electron impact ionization rate β_e decreases with time for electron temperatures smaller than 25 eV. For $T_e > 25$ eV, the rate increases. The relative rate change is small for $T_e < 50$ eV; it peaks and remains approximately constant at temperatures 200–600 eV. It takes about 0.10 year, 0.06 year, 0.05 year, and 0.04 year to increase the electron impact ionization rate, β_e, by 1% for electron temperatures 45 eV, 70 eV, 92 eV, and 180 eV, respectively. In other words, electron impact ionization rates would increase in 1 year by approximately 10%, 16%, 20%, and 25% for such electron temperatures, respectively.

It takes several years for the solar wind plasma to convect through the heliosheath and reach the distant heliotail. Consequently, if the effective electron temperature $T_e > 50$ eV, then the already dominating electron

impact ionization rate may increase substantially, for example, double, in a control volume of the heliosheath plasma as it flows to the tail. Such an increase would be especially pronounced if initial electron temperatures are 100 eV or higher.

4. Discussion and Conclusions

As shown above, photoionization alone could mass-load plasma flows by 10–20% in the heliosheath. The relative magnitude of this effect near the heliopause where the plasma flow slows down would be significantly larger. At the same time, global heliospheric modeling often disregards photoionization beyond the termination shock while emphasizes its importance to closer to the Sun heliocentric distances [e.g., *Zank et al.*, 2009; *Alouani-Bibi et al.*, 2011; *Ratkiewicz et al.*, 2012; *Heerikhuisen et al.,* 2014]. It is clear that the effect of photoionization is noticeable, and models could account for the resulting mass loading of plasma flows in a straightforward way.

Figures 3 and 4 show that electron impact ionization could be significantly larger than photoionization in the heliosheath, and its rate would grow with time, especially if $T_e > 50$ eV. Inclusion of the process into models faces major uncertainties and challenges, however. The formulated concept of heliosphere ENA imaging specifically pointed out lack of knowledge of "how the solar wind energy is redistributed between the proton and electron components of the postshock plasma" [*Gruntman et al.*, 2001] downstream of the termination shock. There is no definitive and validated by measurements answer to this question yet, which is fundamentally important for understanding ionization in the heliosheath.

The plasma instrument on Voyager 2 directly measured velocities of the bulk solar wind plasma across the termination shock and in the heliosheath [*Richardson et al.*, 2008; *Richardson and Wang*, 2012; *Richardson and Decker*, 2014, 2015]. About 200 days before the termination shock crossing, the solar wind velocity was observed to be $V_{SW} \approx 380$ km s^1 which corresponded to proton kinetic energy of 750 eV. The flow then slowed down to about 310 km s^{-1}, or 500 eV per proton, immediately upstream of the termination shock. Downstream of the shock, the velocity dropped to about 120 km s^{-1} and the corresponding 80 eV energy per proton. At the same time, Voyager 2 measured increase of the proton temperature across the shock to ~10^5 K, with the corresponding average energy of proton thermal motion about 13 eV.

So about 650 eV of energy per each original solar wind (nonpickup), proton was transferred in the shock transition to the nonthermal proton population, solar wind electrons, plasma waves, and acceleration of high-energy particles. How exactly this transferred energy is partitioned among these possibilities is an important key to understanding the details of the heliospheric interaction.

Most of energy density (and pressure) in the heliosheath plasma is carried by nonthermal ($E > 0.5$ keV) protons [*Funsten et al.*, 2009b; *Krimigis et al.*, 2009; *Roelof et al.*, 2010; *Schwadron et al.*, 2011]. These particles thus govern to a significant degree the dynamics and plasma flow pattern in the heliosheath while most of the plasma mass (inertia), as Voyager 2 measurements show [*Richardson and Decker*, 2015], is in relatively low temperature (4×10^4–10^5 K) denser bulk solar wind protons. Obtaining nonthermal proton characteristics from the observed by IBEX-Hi ENA intensities in the 0.5–6.0 keV energy range involves accounting for known motion of the observer and a priori unknown motion of the heliosheath plasma [*Gruntman et al.*, 2001; *McComas et al.*, 2010; *Roelof et al.*, 2012], often described as the Compton-Getting effect [*Compton and Getting*, 1935]. For the purposes of estimates in this work, one can disregard such corrections.

Consider a heliosheath of depth L uniformly filled with interstellar hydrogen atoms and ENA-producing protons with the number densities n_0 and n_p, respectively, that are at rest with respect to the observer at 1 AU. For a proton population with an isotropic velocity distribution, the differential (per energy) ENA intensity $F_{ENA}(E)$ is

$$F_{ENA}(E) = \frac{1}{4\pi} \left(\frac{2}{m_p}\right)^{1/2} n_p n_0 \, q(E) \, L \, p(E) \, E^{1/2} f(E),$$

where $q(E)$ is the energy-dependent cross section of proton charge exchange on hydrogen atoms, $p(E)$ is the energy-dependent probability for an ENA to reach the observer without loss, and m_p is the proton mass [e.g., *Gruntman*, 1992, 1997]. Here $f(E)$ is the energy distribution of protons normalized as

$$\int_{E_{MIN}}^{E_{MAX}} f(E) \mathrm{d}E = 1.$$

We limit our consideration to nonthermal protons and ENAs with energies between $E_{MIN} = 0.5$ keV and $E_{MAX} = 6.0$ keV observed by IBEX-Hi [*Funsten et al.*, 2009b]. For a simplified case of ENAs approaching with a constant velocity, V_{ENA}, the observer at the heliocentric distance $R_0 = 1$ AU along radial trajectories, the survival probability is

$$p(E) = \exp\left(-\frac{\beta_E R_0}{V_{ENA}}\right),$$

where $\beta_E = \beta_E(V_{ENA})$ is the total (photoionization and charge exchange on solar wind protons) loss rate of ENAs at 1 AU and $E = m_p V_{ENA}^2/2$.

One can then express the energy distribution of protons as

$$f(E) = \left(\frac{m_p}{2}\right)^{1/2} \frac{4\pi}{\delta}\, \eta(E),$$

where the parameter $\delta = n_p n_0 L$ characterizes the ENA-emitting region of the heliosheath and the energy-dependent function $\eta(E)$ is

$$\eta(E) = \frac{F_{ENA}(E)}{q(E)\, p(E)\, E^{1/2}}.$$

The function $\eta(E)$ and its integral I_η over energies of interest,

$$I_\eta = \int_{E_{MIN}}^{E_{MAX}} \eta(E) dE,$$

are obtained from the measured ENA intensities $F_{ENA}(E)$. Noting the normalization of the energy distribution $f(E)$, one can determine the parameter δ from the observations as

$$\delta = 4\pi \left(\frac{m_p}{2}\right)^{1/2} I_\eta.$$

The IBEX-Hi instrument measured average differential ENA intensities, $F_{ENA}(E)$, of 192, 79, 30, 17, and 8.7 $cm^{-2}\, sr^{-1}\, keV^{-1}\, s^{-1}$ in energy passbands centered, respectively, on 0.7, 1.1, 1.7, 2.7, and 4.3 keV [*Funsten et al.*, 2009b]. The intensities can be approximated by a power law $F \propto E^{-\kappa}$ with the spectral index $\kappa \approx 1.75$. Assuming the photoionization rate $\beta_{S,0} = 1.0 \times 10^{-7}\ s^{-1}$ at 1 AU and using the energy-dependent proton-hydrogen atom charge exchange cross section [*Barnett*, 1990], one obtains

$$\delta \approx 3.8 \times 10^{10}\ cm^{-5} \approx 0.0025\ cm^{-6} AU$$

for the measured heliospheric ENA intensities in the 0.5–6.0 keV range.

For the interstellar hydrogen atom number density $n_0 = 0.18\ cm^{-3}$ adopted in this work and the characteristic thickness of the heliosheath $L = 100$ AU, one obtains the estimate of the number density of nonthermal protons producing 0.5–6.0 keV ENAs to be $n_p = \delta/(n_0 L) \approx 1.4 \times 10^{-4}\ cm^{-3}$. This number density is about one tenth of the plasma number density in the heliosheath which is consistent with the expected abundances of pickup protons in the supersonic solar wind upstream of the termination shock. The average energy ε_p of ENA-producing protons observed by IBEX-Hi is

$$\varepsilon_p = \int f(E) E\, dE \Big/ \int f(E) dE \approx 1300\ eV.$$

Before crossing the termination shock, each proton in the supersonic solar wind carried kinetic energy 750 eV. Pickup protons had additional kinetic energy, in the rest frame of the supersonic solar wind, of about 1 keV per proton. Therefore, their total energy was 1.75 keV per a pickup proton. The estimated average energy $\varepsilon_p \approx 1.3$ keV of nonthermal protons in the heliosheath suggests that the pickup protons may account for the observed by IBEX-Hi heliospheric ENA fluxes without addition of any energy from the bulk (nonpickup) solar wind protons. Note that if these protons acquired some extra energy, it could have also occurred prior to crossing of the termination shock in the region within 1 AU upstream from it. There, the supersonic solar wind slowed down, as observed by Voyager 2 [*Richardson et al.*, 2008], from 380 km s^{-1} to 310 km s^{-1} which corresponded to release of about 250 eV of energy per proton.

To summarize, the observed by IBEX-Hi heliospheric ENAs with 0.5–6.0 keV energies do not seem to require transfer of energy from the bulk solar wind protons to ENA-producing nonthermal proton populations, and the abundance of the latter corresponds to that of the pickup protons in the solar wind before crossing of the termination shock. The energy balance then suggests that the measured by Voyager 2 "lost" 650 eV energy per each proton of the bulk solar wind to be transferred to other plasma components and energetic particles in the termination shock transition. Determining the fraction of this energy imparted to plasma electrons downstream of the shock—that was [*Gruntman et al.*, 2001] and remains unknown and poorly constrained —may hold a key to accurate description of the processes in the heliosheath. In addition, it is not known how representative is the termination shock transition observed by Voyager 2, as orientations of the magnetic field and solar wind velocities could vary. Note that for higher-solar wind velocities characteristic for ecliptic polar regions in solar minima, the transferred energy may be as large as 2 keV per bulk solar wind proton, significantly larger than under the conditions encountered by Voyager 2.

The termination shock accelerates ions to high energies [e.g., *Zank et al.*, 1996]. It was also observed long ago [*Isenberg and Feldman*, 1997] that interplanetary solar wind shocks generate populations of 30–150 eV electrons. So it is not excluded that the termination shock also produces copious higher-energy electrons that are carried by the heliosheath plasma. In contrast to the LISM where mean free paths for electron-electron collisions are under 1 AU, the heliosheath plasma is essentially not Coulomb collisional. Therefore, energy distributions of heliosheath electrons could also deviate from being Maxwellian. Very few publications that tried to theoretically consider properties of electrons in the termination shock transition and beyond pointed to fundamental unresolved difficulties in describing such processes [e.g., *Chalov and Fahr*, 2013; *Chashei and Fahr*, 2013; *Izmodenov et al.*, 2014]. It is important that no reliable in situ measurements of electrons at the termination shock and in the heliosheath exist or are expected in the foreseeable future.

Therefore, one arrives at two contrasting possibilities based on energy conservation in the shock transition, one with negligibly small and the other with nonnegligible fractions of the bulk solar wind energy imparted to electrons in the heliosheath. In the former case, effective electron temperature would be only a few eV or smaller with the resulting electron impact ionization of interstellar hydrogen smaller than that of photoionization (Figure 3). In the latter case, electron impact ionization would dominate and it could be an order of magnitude higher than photoionization for electron temperatures 50 eV or higher. The temperature dependence of electron impact ionization (Figure 3, bottom) suggests that its effects would be about the same for the effective electron temperature raised in the shock transition to any value in the 60–400 eV range. Significant electron temperatures may also introduce additional modeling complications caused by high and anisotropic thermal conductivity in the heliosheath plasma flow [e.g., *Izmodenov et al.*, 2014].

Photoionization alone could result in mass loading of about 10% of the heliosheath plasma flow entering the downwind hemisphere at $\theta = 90°$ (Figure 1) and up to about 20% further down in the heliosphere tail. This effect would be especially pronounced for plasma flow that initially streams into the upwind hemisphere and then being slowly convected along the heliopause boundary toward the tail. If electron temperature increases to 50 eV or higher in the termination shock transition, then electron impact ionization would roughly double the number density of the heliosheath plasma entering the downwind hemisphere. In turn, such mass loading should significantly slow down the plasma flow. In the absence of Maxwellization of electrons, ionization of hydrogen atoms would result in complex energy distributions of plasma electrons, further complicating description of the heliosheath.

The interstellar hydrogen ionization effect is essentially nonlinear as the resulting mass loading slows down the plasma flow, causes compression, and increases importance of continuing ionization. In addition, the heliosheath plasma continuously emits ENAs and thus losses its momentum and energy, reducing velocities of plasma flows. The rate of electron impact ionization also increases as electrons are added to the heliosheath plasma. As a result, one could expect a significant ionization effect on the heliosheath plasma, especially severe near the heliopause. The distant heliospheric tail is another region where ionization would strongly modify plasma flow properties and ENA emissions.

One could speculate that temporal solar cycle variations of the global solar wind might create conditions, especially near the heliopause, where a plasma flow could come practically to rest at some regions of the heliosheath. Localized plasma with near-zero flow velocities could first produce enhanced ENA emissions as it piles up and becomes denser and then its intensity decreases as the nonthermal proton population is depleted, the latter process sometimes described as plasma "aging" [*Gruntman et al.*, 2009].

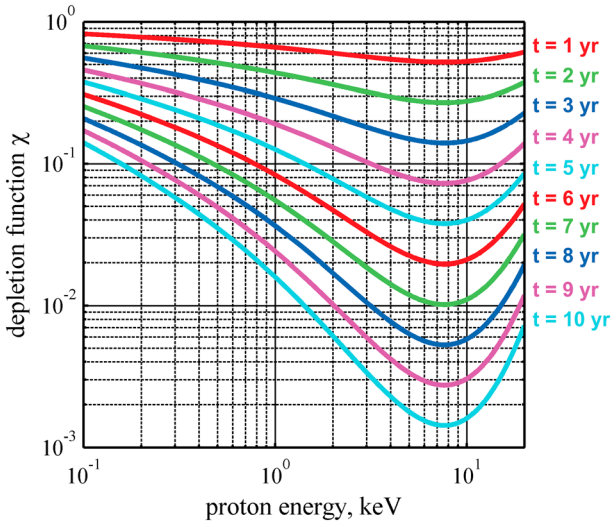

Figure 5. Energy dependence of the depletion function $\chi(E,t)$ for time intervals from 1 to 10 years; the interstellar hydrogen number density is $n_0 = 0.18\ \mathrm{cm}^{-3}$.

The number density of protons with energy E and produced by them ENA fluxes decreases by the energy-dependent depletion, or aging, factor,

$$\chi(E,t) = \exp\left[-n_0\, q(E)\, \left(2E/m_p\right)^{1/2}\, t\right],$$

as a function of time t due to charge exchange on the background gas. Figure 5 shows energy dependence of the aging factor for the adopted in this work, interstellar hydrogen number density $n_0 = 0.18\ \mathrm{cm}^{-3}$ for time intervals from 1 to 10 years.

Consider, for example, protons with energy $E = 3$ keV. After 7 years, their population would decrease by a factor of 50 and ENA fluxes at this energy practically vanish. Note that a flow with a velocity of 100 km s^{-1} covers a distance of 21 AU in 1 year. So plasma with typical flow velocities 150 km s^{-1}, as those observed by Voyager 2 in the heliosheath [*Richardson and Decker*, 2015], would move by 220 AU in 7 years which is about the characteristic size of the heliosphere. Therefore, the solar wind plasma initially flowing into the upwind hemisphere would contribute very little to ENA fluxes at such energies when it reaches the heliospheric tail at distances of 150 AU from the Sun and beyond.

Figure 5 also suggests that the effect of aging of ENA-producing proton populations is highly sensitive to slowing down of the plasma flow in the heliosheath and thus strongly depends on ionization efficiency of interstellar hydrogen. One can see, as an example, that just 1 year increase of the age of protons at 3 keV, from 4 to 5 years, would decrease ENA intensities at this energy by a factor of 2. Mass loading due to photoionization alone could make the plasma "older" to such a degree in parts of the heliosheath. Therefore, omitting photoionization in global heliosphere modeling could lead to similar errors in predicted ENA intensities and make comparison with the experimentally obtained ENA images difficult and uncertain. In addition, unaccounted for electron impact ionization could be much more efficient than photoionization, perhaps by an order of magnitude, with the corresponding effect on ENA fluxes.

The IBEX-Hi instrument observed ENA emissions with complicated and yet to be explained time history. In particular, changes in localized intensities in the part of the ribbon (also with differing spectral properties of ENAs) known as the "knot" [*Funsten et al.*, 2009b; *McComas et al.*, 2010; 2012, 2014] could be a manifestation of complex variations of plasma flows driven, in part, by interstellar hydrogen ionization.

Electron impact ionization would become prominent in the heliosheath if only a small fraction, just 10%, of the energy carried by the bulk solar wind plasma upstream of the termination shock is transferred to electrons. This small energy transfer should thus not alter the energy available for ion acceleration mechanisms at the termination shock [e.g., *Zank*, 1999] or affect interpretation of energy spectra of protons with >20 keV measured in situ by Voyager spacecraft [e.g., *Decker et al.*, 2008; *Stone et al.*, 2008, 2013; *Krimigis et al.*, 2013].

In other words, existing observations and conservation of energy do not seem to preclude transfer of a fraction of bulk solar wind energy to heliosheath electrons that would be sufficient to significantly affect plasma flows. Therefore, inclusion of electron impact ionization as well as photoionization of interstellar hydrogen into heliospheric models and computer simulations is indispensable for understanding the heliosheath.

Global heliospheric models are already highly complex which obscures relative importance of various physical processes involved. Dedicated parametric studies of the effects of ionization on observable ENA fluxes could advance understanding of the interaction. Present descriptions of the heliospheric interaction almost exclusively rely on the Euler variables for flow fields. Following evolution of plasma parameters in the

Lagrange variables for control mass along flow lines could provide important insight and better understanding of the heliosheath plasma and determine effects of various physical processes on predicted ENA images.

The presented estimates clearly show that, in addition to solar photoionization, electrons could play a major and consequential role in shaping the plasma flow in the heliosheath and producing heliospheric ENA fluxes. Advancing theoretical understanding of energy transfer to electrons in the termination shock transition is essential for accurate accounting of ionization of interstellar hydrogen and its effect on the heliosheath plasma. It is also important to quantitatively determine how absence of measurable electron fluxes by the Voyager 2 plasma instrument beyond the termination shock constrains possible effective temperatures and velocity distributions of electrons. In the longer term, in situ measurement of electrons should be among top priorities for the future Interstellar Probe mission [*Mewaldt and Liewer*, 2001; *McNutt et al.*, 2003, 2004; *Gruntman*, 2004; *Fiehler and McNutt,* 2006; *Wimmer-Schweingruber et al.*, 2009; *McNutt et al.*, 2011].

Acknowledgments
This work is supported, in part, by NASA's IBEX program. I want to thank John Richardson for discussion of measurements by the plasma instrument on Voyager 2. All data for this paper are cited and referred to in the text and in the reference list, respectively.

Yuming Wang thanks one anonymous reviewer for assisting in the evaluation of this paper.

References

Alouani-Bibi, F., M. Opher, D. Alexashov, V. Izmodenov, and G. Toth (2011), Kinetic versus multi-fluid approach for interstellar neutrals in the heliosphere: Exploration of the interstellar magnetic field effects, *Astrophys. J.*, *734*, 45, doi:10.1088/0004-637X/734/1/45.

Banks, P. M. (1971), Interplanetary hydrogen and helium from cosmic dust and the solar wind, *J. Geophys. Res.*, *76*, 4341–4348, doi:10.1029/JA076i019p04341.

Baranov, V. B., and Y. G. Malama (1993), Model of the Solar Wind interaction with the Local Interstellar Medium: Numerical solution of self-consistent problem, *J. Geophys. Res.*, *98*(A9), 15,157–15,163, doi:10.1029/93JA01171.

Baranov, V. B., and Y. G. Malama (1996), Axisymmetric self-consistent model of the solar wind interaction with the LISM: Basic results and possible ways of development, *Space Sci. Rev.*, *78*, 305–316, doi:10.1007/bf00170817.

Barnett, C. F. (Ed.) (1990), *Atomic Data for Fusion. Volume 1: Collisions of H, H2, He, and Li Atoms and Ions with Atoms and Molecules*, ORNL-6086, Oak Ridge Natl. Lab., Oak Ridge, Tenn.

Bleszynski, S., S. Grzedzielski, D. Rucinski, and J. Jakimec (1992), Expected fluxes of about 1 keV neutral H atoms in interplanetary space - Comparison with the U.V. background and possibility of detection, *Planet. Space Sci.*, *40*, 1525–1533, doi:10.1016/0032-0633(92)90049-T.

Bochsler, P., H. Kucharek, E. Moebius, M. Bzowski, J. M. Sokol, L. Didkovsky, and S. Wieman (2014), Solar photoionization rates for interstellar neutrals in the inner heliosphere: H, He, O, and Ne, *Astrophys. J. Suppl.*, *210*, 12, doi:10.1088/0067-0049/210/1/12.

Bridge, H. S., J. W. Belcher, R. J. Butler, A. J. Lazarus, A. M. Mavretic, J. D. Sullivan, G. L. Siscoe, and V. M. Vasyliunas (1977), The plasma experiment on the voyager mission, *Space Sci. Rev.*, *21*, 259–287, doi:10.1007/BF00211542.

Burlaga, L. F., N. F. Ness, and E. C. Stone (2013), Magnetic field observations as voyager 1 entered the heliosheath depletion region, *Science*, *341*, 147–150, doi:10.1126/science.1235451.

Chalov, S. V., and H. J. Fahr (2013), The role of solar wind electrons at the solar wind termination shock, *Mon. Not. R. Astron. Soc.*, *433*, L40–L43, doi:10.1093/mnrasl/slt052.

Chalov, S. V., D. B. Alexashov, D. McComas, V. V. Izmodenov, Y. G. Malama, and N. Schwadron (2010), Scatter-free pickup ions beyond the heliopause as a model for the interstellar boundary explorer ribbon, *Astrophys. J. Lett.*, *716*(2), L99–L102, doi:10.1088/2041-8205/716/2/L99.

Chashei, I. V., and H. J. Fahr (2013), On the electron temperature downstream of the solar wind termination shock, *Ann. Geophys.*, *31*, 1205–1212, doi:10.5194/angeo-31-1205-2013.

Compton, A. H., and I. Getting (1935), An apparent effect of galactic rotation on the intensity of cosmic rays, *Phys. Rev.*, *47*, 817–821, doi:10.1103/PhysRev.47.817.

Decker, R. B., S. M. Krimigis, E. C. Roelof, M. E. Hill, T. P. Armstrong, G. Gloeckler, D. C. Hamilton, and L. J. Lanzerotti (2005), Voyager 1 in the foreshock, termination shock, and heliosheath, *Science*, *309*(5743), 2020–2024, doi:10.1126/science.1117569.

Decker, R. B., S. M. Krimigis, E. C. Roelof, M. E. Hill, T. P. Armstrong, G. Gloeckler, D. C. Hamilton, and L. J. Lanzerotti (2008), Mediation of the solar wind termination shock by non-thermal ions, *Nature*, *454*, 67–70, doi:10.1038/nature070307.

Fahr, H. J. (1968), Neutral corpuscular energy flux by charge-transfer collisions in the vicinity of the Sun, *Astrophys. Space Sci.*, *2*, 496–503, doi:10.1007/BF02175924.

Fahr, H. J., T. Kausch, and H. Scherer (2000), A 5-fluid hydrodynamic approach to model the solar system-interstellar medium interaction, *Astron. Astrophys.*, *357*, 268–282.

Fahr, H.-J., H. Fichtner, and K. Scherer (2007), Theoretical aspects of energetic neutral atoms as messengers from distant plasma sites with emphasis on the heliosphere, *Rev. Geophys.*, *45*, RG4003, doi:10.1029/2006RG000214.

Fiehler, D. I., and R. L. McNutt Jr. (2006), Mission design for the innovative interstellar explorer vision mission, *J. Spacecr.*, *43*, 1239–1247, doi:10.2514/1.20995.

Funsten, H. O., et al. (2009a), The Interstellar Boundary Explorer High Energy (IBEX-Hi) neutral atom imager, *Space Sci. Rev.*, *146*, 75–103, doi:10.1007/s11214-009-9504-y.

Funsten, H. O., et al. (2009b), Structures and spectral variations of the outer heliosphere in IBEX energetic neutral atom maps, *Science*, *326*, 964–966, doi:10.1126/science.1180927.

Gruntman, M. (1980), The neutral component of the Solar Wind at Earth's orbit, *Kosm. Issled. (Cosmic Res.)*, *18*(4), 649–651.

Gruntman, M. (1982), Effect of neutral component of solar wind on the interaction of the Solar system with the interstellar gas flow, *Sov. Astron. Lett.*, *8*(1), 24–26.

Gruntman, M. (1992), Anisotropy of the energetic neutral atom flux in the heliosphere, *Planet. Space Sci.*, *40*, 439–445, doi:10.1016/0032-0633(92)90162-H.

Gruntman, M. (1994), Neutral solar wind properties: Advance warning of major geomagnetic storms, *J. Geophys. Res.*, *99*, 19,213–19,227, doi:10.1029/94JA01571.

Gruntman, M. (1997), Imaging of space plasmas in energetic neutral atom fluxes, *Rev. Sci. Instrum.*, *68*(10), 3617–3656, doi:10.1063/1.1148389.

Gruntman, M. (2004), Instrumentation for interstellar exploration, *Adv. Space Res.*, *34*(1), 204–212, doi:10.1016/j.asr.2003.04.064.
Gruntman, M., and V. B. Leonas (1983), Neutral Solar Wind. Possibility of Experimental Study Preprint 825 (42 pp.), Space Research Institute (IKI), USSR Academy of Sciences, Moscow. [Available at http://astronauticsnow.com/mg_pubs/gruntman_preprint-825-iki-1983.pdf.]
Gruntman, M., and V. B. Leonas (1986), Possibility of experimental study of energetic neutral atoms in interplanetary space, Preprint-1109 (22 pp.), Space Research Institute (IKI), USSR Academy of Sciences, Moscow. [Available at http://astronauticsnow.com/mg_pubs/gruntman_preprint-1109-iki-1986.pdf.]
Gruntman, M., S. Grzedzielski, and V. B. Leonas, (1990), Neutral Solar Wind Experiment, in *Physics of the Outer Heliosphere*, *Proc. 1st COSPAR Colloq.*, edited by S. Grzedzielski and D. E. Page, pp. 355–358, Pergamon Press, Oxford, U. K., doi:10.1016/B978-0-08-040780-7.50059-2.
Gruntman, M., E. C. Roelof, D. G. Mitchell, H. J. Fahr, H. O. Funsten, and D. J. McComas (2001), Energetic neutral atom imaging of the heliospheric boundary region, *J. Geophys. Res.*, *106*, 15,767–15,781, doi:10.1029/2000JA000328.
Gruntman, M., E. C. Roelof, D. J. McComas, H. O. Funsten, S. M. Krimigis, and D. G. Mitchell (2009), Physical Processes in the Heliospheric Interface Region and their Implications for ENA Images, SH21B-1518, AGU, Fall Meeting.
Heerikhuisen, J., N. V. Pogorelov, G. P. Zank, G. B. Crew, P. C. Frisch, H. O. Funsten, P. H. Janzen, D. J. McComas, D. B. Reisenfeld, and N. A. Schwadron (2010), Pick-up ions in the outer heliosheath: A possible mechanism for the interstellar boundary explorer ribbon, *Astrophys. J. Lett.*, *708*, L126–L130, doi:10.1088/2041-8205/708/2/L126.
Heerikhuisen, J., E. J. Zirnstein, H. O. Funsten, N. V. Pogorelov, and G. P. Zank (2014), The effect of new interstellar medium parameters on the heliosphere and energetic neutral atoms from the interstellar boundary, *Astrophys. J.*, *784*, 73, doi:10.1088/0004-637X/784/1/73.
Holzer, T. E. (1977), Neutral hydrogen in interplanetary space, *Rev. Geophys. Space Phys.*, *15*, 467–490, doi:10.1029/RG015i004p00467.
Hsieh, K. C., and M. A. Gruntman (1993), Viewing the outer heliosphere in energetic neutral atoms, *Adv. Space Res.*, *13*(6), 131–139, doi:10.1016/0273-1177(93)90402-W.
Hsieh, K. C., K. L. Shih, J. R. Jokipii, and M. Gruntman (1991), Sensing the solar-wind termination shock from Earth's orbit, in *Solar Wind Seven*, *Proc. 3rd COSPAR Colloq.*, pp. 365–368, Goslar, Germany, Pergamon, Oxford.
Isenberg, P. A., and W. C. Feldman (1997), Electron-impact ionization of interstellar hydrogen and helium at interplanetary shocks, *Geophys. Res. Lett.*, *22*, 873–875, doi:10.1029/95GL00703.
Izmodenov, V. (2000), Physics and gasdynamics of the heliospheric interface, *Astrophys. Space Sci.*, *274*, 55–69.
Izmodenov, V. V., and V. B. Baranov (2006), Modern multi-component models of the heliospheric interface, in *The Physics of the Heliospheric Boundaries*, *ISSI Sci. Rep. No. 5*, edited by V. Izmodenov and R. Kallenbach, pp. 67–135, ESA-ESTEC, Paris.
Izmodenov, V. V., Y. G. Malama, M. S. Ruderman, S. V. Chalov, D. B. Alexashov, O. A. Katushkina, and E. A. Provornikova (2009), Kinetic-gasdynamic modeling of the heliospheric interface, *Space Sci. Rev.*, *146*, 329–351, doi:10.1007/s11214-009-9528-3.
Izmodenov, V. V., O. A. Katushkina, E. Quemerais, M. Bzowski (2013), distribution of interstellar hydrogen atoms in the heliosphere and backscattered solar lyman-α, in *Cross-Calibration of Far UV Spectra of Solar System Objects and the Heliosphere*, *ISSI Sci. Rep. Ser.*, vol. 13, pp. 7–65, Springer, New York, doi:10.1007/978-1-4614-6384-9_2.
Izmodenov, V. V., D. B. Alexashov, and M. S. Ruderman (2014), Electron thermal conduction as a possible physical mechanism to make the inner heliosphere thinner, *Astrophys. J. Lett.*, *795*, L7, doi:10.1088/2041-8205/795/1/L7.
Izmodenov, V., Y. G. Malama, G. Gloeckler, and J. Geiss (2003), Effects of interstellar and solar wind ionized helium on the interaction of the solar wind with the local interstellar medium, *Astrophys. J. Lett.*, *594*, L59–L62.
Janev, R. K., W. D. Langer, K. Evans, and D. E. Post Jr. (1987), *Elementary Processes in Hydrogen-Helium Plasmas*, *Cross Sect. React. Rate Coeffic.*, Springer, New York.
Janev, R. K., D. Reitler, and U. Samm (2003), Collision Processes in Low-Temperature Hydrogen Plasmas, Berichte des Forschungszentrums Jülich 4105.
Krimigis, S. M., D. G. Mitchell, E. C. Roelof, K. C. Hsieh, and D. J. McComas (2009), Imaging the interaction of the heliosphere with the interstellar medium from Saturn with Cassini, *Science*, *326*, 971–973, doi:10.1126/science.1181079.
Krimigis, S. M., R. B. Decker, E. C. Roelof, M. E. Hill, T. P. Armstrong, G. Gloeckler, D. C. Hamilton, and L. J. Lanzerotti (2013), Search for the exit: Voyager 1 at Heliosphere's border with the Galaxy, *Science*, *341*, 144–147, doi:10.1126/science.1235721.
Malama, Y. G., V. V. Izmodenov, and S. V. Chalov (2006), Modeling of the heliospheric interface: Multi-component nature of the heliospheric plasma, *Astron. Astrophys.*, *445*, 693–701, doi:10.1051/0004-6361:20053646.
McComas, D. J., et al. (2003), Interstellar pathfinder – A mission to the inner edge of the interstellar medium in *Solar Wind Ten: Proceedings. of the Tenth Solar Wind Conference*, *AIP Confe. Proc.* vol. 679., edited by M. Velli, R. Bruno, and F. Malara, pp. 834–837, Am. Instit. Physics, Melville, New York, doi:10.1063/1.1618720.
McComas, D. J., R. W. Ebert, H. A. Elliott, B. E. Goldstein, J. T. Gosling, N. A. Schwadron, and R. M. Skoug (2008), Weaker solar wind from the polar coronal holes and the whole Sun, *Geophys. Res. Lett.*, *35*, L18103, doi:10.1029/2008GL034896.
McComas, D. J., et al. (2009a), IBEX—Interstellar Boundary Explorer, *Space Sci. Rev.*, *146*, 11–33, doi:10.1007/s11214-009-9499-4.
McComas, D. J., et al. (2009b), First global observations of the interstellar interaction from the interstellar boundary explorer, *Science*, *326*, 959–962, doi:10.1126/science.1180906.
McComas, D. J., et al. (2010), Evolving outer heliosphere: Large-scale stability and time variations observed by the Interstellar Boundary Explorer, *J. Geophys. Res.*, *115*, A09113, doi:10.1029/2010JA015569.
McComas, D. J., et al. (2012), The first three years of IBEX observations and our evolving heliosphere, *Astrophys. J. Suppl.*, *203*, 1, doi:10.1088/0067-0049/203/1/1.
McComas, D. J., et al. (2014), IBEX: The First Five Years (2009–2013), *Astrophys. J. Suppl.*, *213*(2), 20, doi:10.1088/0067-0049/213/2/20.
McNutt, R. L., Jr., G. B. Andrews, J. V. McAdams, R. E. Gold, A. Santo, D. Oursler, K. J. Heeres, M. Fraeman, and B. D. Williams (2003), Low-cost interstellar probe, *Acta Astronaut.*, *52*, 267–279, doi:10.1016/S0094-5765(02)00166-2.
McNutt, R. L., Jr., et al. (2004), A realistic interstellar explorer, *Adv. Space Res.*, *34*, 192–197, doi:10.1016/j.asr.2003.03.053.
McNutt, R. L., Jr., M. Gruntman, S. M. Krimigis, E. C. Roelof, and R. F. Wimmer-Schweingruber (2011), Interstellar probe: Impact of the voyager and IBEX results on science and strategy, *Acta Astronaut.*, *69*, 767–776, doi:10.1016/j.actaastro.2011.05.024.
Mewaldt, R., and P. Liewer (2001), Scientific payload for an Interstellar Probe mission, in *The Outer Heliosphere: The Next Frontiers*, *Proc. of COSPAR Colloq*, edited by K. Scherer et al., pp. 451–464, Pergamon, Oxford, doi:10.1016/S0964-2749(01)80105-0.
Moebius, E., G. Gloeckler, M. Gruntman, and H. Fahr (1998), A Local Interstellar Medium Explorer (LIME) mission to set a benchmark with in-situ measurements from 1–3 AU, *Eos Trans. AGU*, *79*(17), Spring Meet. Suppl., p. S269, April 28.
Opher, M., E. C. Stone, and P. C. Liewer (2006), The effects of a local interstellar magnetic field on Voyager 1 and 2 observations, *Astrophys. J. Lett.*, *640*, L71–L74, doi:10.1086/503251.
Opher, M., J. F. Drake, B. Zieger, and T. Gombosi (2015), Magnetized jets driven by the Sun: the structure of the heliosphere revisited, *Astrophys. J. Lett.*, *800*, L28, doi:10.1088/2041-8205/800/2/L28.

Patterson, T. N. L., K. S. Johnson, and W. B. Hanson (1963), The distribution of interplanetary hydrogen, *Planet. Space Sci.*, *11*, 767–778, doi:10.1016/0032-0633(63)90189-2.

Pogorelov, N. V., J. Heerikhuisen, and G. P. Zank (2008), Probing heliospheric asymmetries with an MHD-kinetic model, *Astrophys. J. Lett.*, *675*, L41–L44, doi:10.1086/529547.

Ratkiewicz, R., M. Strumik, and J. Grygorczuk (2012), The effects of local interstellar magnetic field on energetic neutral atom sky maps, *Astrophys. J.*, *756*, 3, doi:10.1088/0004-637X/756/1/3.

Richardson, J. D., and R. B. Decker (2014), Voyager 2 observations of plasmas and flows out to 104 AU, *Astrophys. J.*, *792*, 126, doi:10.1088/0004-637X/792/2/126.

Richardson, J. D., and R. B. Decker (2015), Plasma and flows in the heliosheath, Voyager, IBEX, and the Interstellar Medium, *J. Phys. Conf. Ser.*, *577*, 012021, doi:10.1088/1742-6596/577/1/012021.

Richardson, J. D., and C. Wang (2012), Voyager 2 observes a large density increase in the heliosheath, *Astrophys. J. Lett.*, *759*, L19, doi:10.1088/2041-8205/759/l/L19.

Richardson, J. D., J. C. Kasper, C. Wang, J. W. Belcher, and A. J. Lazarus (2008), Cool heliosheath plasma and deceleration of the upstream solar wind at the termination shock, *Nature*, *454*, 71–74, doi:10.1038/nature07024.

Roelof, E. C. (1992), Imaging heliospheric shocks using energetic neutral atoms, in *Solar Wind Seven*, *Proceedings of the 3rd COSPAR Colloquium*, pp. 385–390, Goslar, Germany, 1991, Pergamon, Oxford, doi:10.1016/b978-0-08-042049-3.50081-8.

Roelof, E. C., S. M. Krimigis, D. G. Mitchell, R. B. Decker, J. D. Richardson, M. Gruntman, and H. O. Funsten (2010), Implications of generalized rankine-hugoniot conditions for the PUI population at the voyager 2 termination shock, in *Pickup Ions Throughout the Heliosphere And Beyond*, *Proc. 9th Ann. Intern. Astrophys. Conf., AIP Conf. Proc.*, vol. 1302, pp. 133–141, Am. Inst. of Phys., New York, doi:10.1063/1.3529960.

Roelof, E. C., S. M. Krimigis, D. G. Mitchell, R. B. Decker, and K. Dialynas (2012), Cassini ENA images of the heliosheath and Voyager "ground truth": Thickness of the heliosheath, *AIP Conf. Proc.*, *1436*, 239–244, doi:10.1063/1.4723614.

Scherer, K., H. Fichtner, H.-J. Fahr, M. Bzowski, and S. E. S. Ferreira (2014), Ionization rates in the heliosheath and in astrosheaths. Spatial dependence and dynamical relevance, *Astron. Astrophys.*, *563*, A69, doi:10.1051/0004-6361/201321151.

Schwadron, N. A., et al. (2009), Comparison of Interstellar Boundary Explorer Observations with 3-D Global Heliospheric Models, *Science*, *326*, 966–968, doi:10.1126/science.1180986.

Schwadron, N. A., et al. (2011), Separation of the interstellar boundary explorer ribbon from globally distributed energetic neutral atom flux, *Astrophys. J.*, *731*, 56, doi:10.1088/0004-637X/731/1/56.

Scudder, J. D., E. C. Sittler Jr., and H. S. Bridge (1981), A survey of the plasma electron environment of Jupiter: A view from Voyager, *J. Geophys. Res.*, *86*, 8157–8179, doi:10.1029/JA086iA10p08157.

Sittler, E. C., Jr. (1983), Plasma electron analysis: Voyager plasma science experiment, NASA TM-85307.

Stone, E. C., A. C. Cummings, F. B. McDonald, B. C. Heikkila, N. Lal, and W. R. Webber (2005), Voyager 1 explores the termination shock region and the heliosheath beyond, *Science*, *309*(5743), 2017–2020, doi:10.1126/science.1117684.

Stone, E. C., A. C. Cummings, F. B. McDonald, B. C. Heikkila, N. Lal, and W. R. Webber (2008), An asymmetric solar wind termination shock, *Nature*, *454*, 71–74, doi:10.1038/nature07022.

Stone, E. C., A. C. Cummings, F. B. McDonald, B. C. Heikkila, N. Lal, and W. R. Webber (2013), Voyager 1 Observes Low-Energy Galactic Cosmic Rays in a Region Depleted of Heliospheric Ions, *Science*, *341*, 150–153, doi:10.1126/science.1236408.

Wimmer-Schweingruber, R. F., R. McNutt, N. Schwadron, P. C. Frisch, M. Gruntman, P. Wurz, E. Valtonen, and The IHP/HEX Team (2009), Interstellar heliospheric probe/heliospheric boundary explorer mission – A mission to the outermost boundaries of the solar system, *Exp. Astron.*, *24*, 9–46, doi:10.1007/s10686-008-9134-5.

Zank, G. P. (1999), Interaction of the solar wind with the Local Interstellar Medium: A theoretical perspective, *Space Sci. Rev.*, *89*, 413–6888, doi:10.1023/A:1005155601277.

Zank, G. P., H. L. Pauls, I. H. Cairns, and G. M. Webb (1996), Interstellar pickup ions and quasi-perpendicular shocks: Implications for the termination shock and interplanetary shocks, *J. Geophys. Res.*, *101*, 457–478, doi:10.1029/95JA02860.

Zank, G. P., N. V. Pogorelov, J. Heerikhuisen, H. Washimi, V. Florinski, S. Borovikov, I. Kryukov, and H. R. Mueller (2009), Physics of the Solar Wind – Local Interstellar Medium interaction: Role of magnetic fields, *Space Sci. Rev.*, *146*, 295–327, doi:10.1007/s11214-009-9497-6.